USGS
science for a changing world

Prepared for the National Aeronautics and Space Administration

Geologic Map of MTM 35337, 40337, and 45337 Quadrangles, Deuteronilus Mensae Region of Mars

By Frank C. Chuang and David A. Crown

Pamphlet to accompany
Scientific Investigations Map 3079

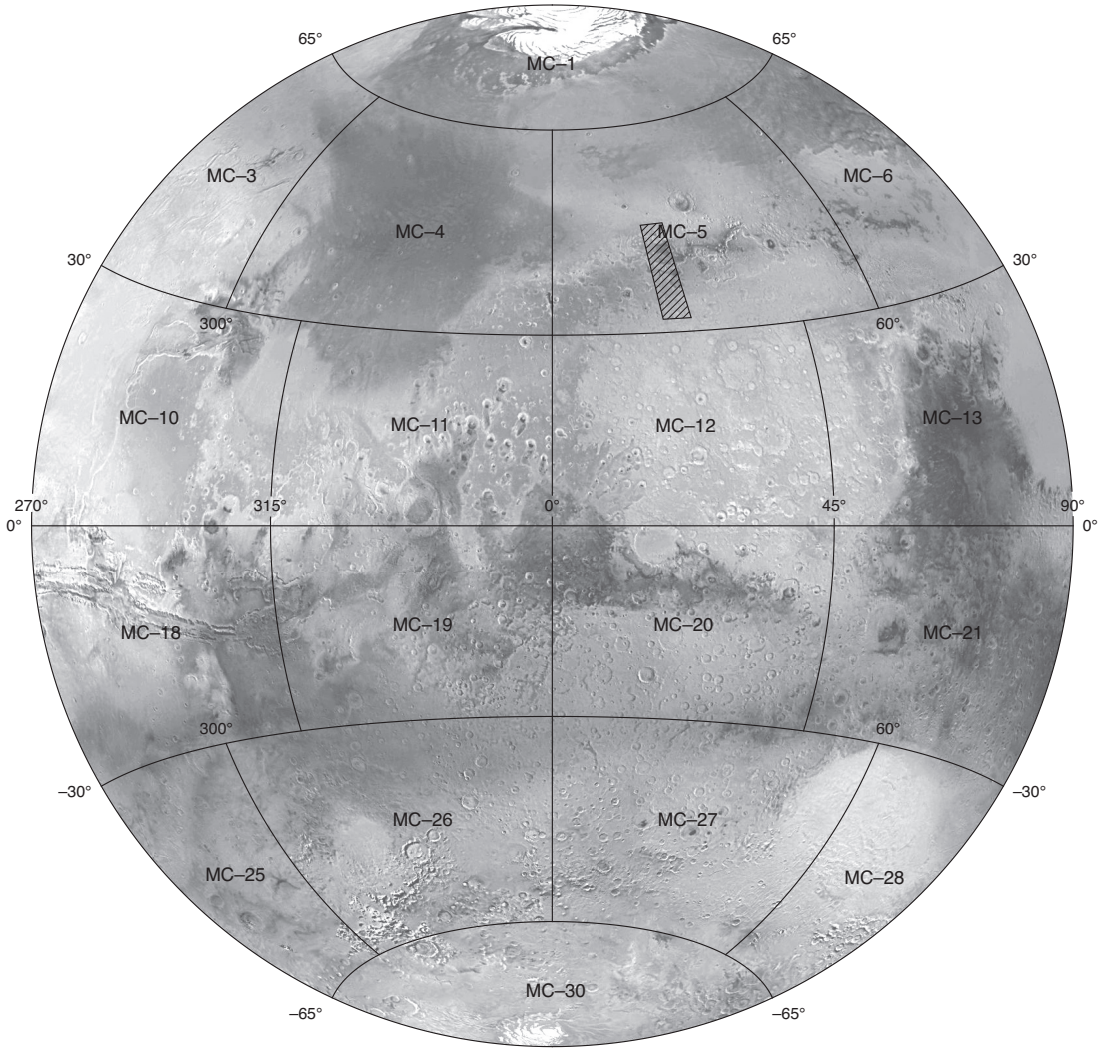

2009

U.S. Department of the Interior
U.S. Geological Survey

INTRODUCTION

Deuteronilus Mensae, first defined as an albedo feature at lat 35.0° N., long 5.0° E., by U.S. Geological Survey (USGS) and International Astronomical Union (IAU) nomenclature, is a gradational zone along the dichotomy boundary (Watters and McGovern, 2006) in the northern mid-latitudes of Mars. The boundary in this location includes the transition from the rugged cratered highlands of Arabia Terra to the northern lowland plains of Acidalia Planitia (fig. 1). Within Deuteronilus Mensae, polygonal mesas are prominent along with features diagnostic of Martian fretted terrain, including lobate debris aprons, lineated valley fill, and concentric crater fill (Sharp, 1973a; Carr, 1996, 2001). Lobate debris aprons, as well as the valley and crater fill deposits, are geomorphic indicators of ground ice (Squyres, 1978, 1979, 1989; Lucchitta, 1984; Squyres and Carr, 1986), and their concentration in Deuteronilus Mensae is of great interest because of their potential association with Martian climate change (Head and others, 2003, 2005, 2006a,b). The paucity of impact craters on the surfaces of debris aprons and the presence of ice-cemented mantle material (Mustard and others, 2001) imply young (for example, Amazonian) surface ages that are consistent with recent climate change in this region of Mars.

North of Deuteronilus Mensae are the northern lowlands, a potential depositional sink that may have had large standing bodies of water or an ocean in the past (Parker and others, 1989, 1993; Edgett and Parker, 1997; Head and others, 1999; Clifford and Parker, 2001; Kreslavsky and Head, 2002; Carr and Head, 2003; Fairen and others, 2003; Webb, 2004; Ghatan and Zimbelman, 2006). The northern lowlands have elevations that are several kilometers below the ancient cratered highlands with significantly younger surface ages. The morphologic and topographic characteristics of the Deuteronilus Mensae region record a diverse geologic history, including significant modification of the ancient highland plateau and resurfacing of low-lying regions. Previous studies of this region have interpreted a complex array of geologic processes, including eolian, fluvial and glacial activity, coastal erosion, marine deposition, mass wasting, tectonic faulting, effusive volcanism, and hydrovolcanism (see McGill, 2002).

The origin and age of the Martian crustal dichotomy boundary are fundamental questions that remain unresolved at the present time. Several scenarios for its formation, including single and multiple large impact events, have been proposed and debated in the literature (Wilhelms and Squyres, 1984; Frey and Schultz, 1988; McGill, 1989; Schultz and Frey, 1990; McGill and Squyres, 1991, Nimmo and Tanaka, 2005; Andrews-Hanna and others, 2008). Endogenic processes whereby crust is thinned by internal mantle convection (Wise and others 1979; McGill and Dimitriou, 1990; Zuber and others, 2000; Zhong and Zuber, 2001; Zuber, 2001) and tectonic processes have also been proposed (Sleep, 1994, 2000). Planetary accretion models and isotopic data from Martian meteorites suggest that the crust formed very early in Martian history (Solomon and others, 2005). Using populations of quasi-circular depressions extracted from the topography of Mars, other studies suggest that the age difference between the highlands and lowlands could be ~100 m.y. (Frey, 2006). Furthermore, understanding the origin and age of the dichotomy boundary has been made more complicated due to significant erosion and deposition that have modified the boundary and its adjacent regions (Skinner and others, 2004; Irwin and others, 2004; Tanaka and others, 2005; Head and others, 2006a; Rodriguez and others, 2006). The resulting diversity of terrains and features is likely a combined result of ancient and recent events. Detailed geologic analyses of dichotomy boundary zones are important for understanding the spatial and temporal variations in highland evolution. This information, and comparisons to other highland regions, can help elucidate the scale of potential environmental changes.

Previous geomorphic and geologic mapping investigations of the Deuteronilus Mensae region have been completed at local to global scales. The regional geology was first mapped by Lucchitta (1978) at 1:5,000,000 scale using Mariner 9 data. This study concluded that high crater flux early in Martian history formed overlapping craters and basins that were later filled by voluminous lava flows that buried the impacted surface, creating the highlands. After this period of heavy bombardment, fluvial erosion of the highlands formed the canyons and valleys, followed by dissection that created the small mesas and buttes, and later, formation of the steep escarpment marking the present-day northern highland margin. After valley dissection, mass wasting and eolian processes caused lateral retreat of mesas and buttes, followed by eruption of flood lavas that covered parts of the current-day smooth plains and dissected highlands. Based on Viking Orbiter data, Greeley and Guest (1987) mapped the region at 1:15,000,000 scale and divided the map region into Noachian highland units, Hesperian ridged plains, older channel materials, and young slide materials (which include both discrete debris aprons and adjacent plains). Collapse and redistribution of highland materials occurred locally from the Late Hesperian into the Amazonian. Geologic mapping at 1:1,000,000 scale of MTM quadrangles 30332, 35332, 40332, and 45332 in the Deuteronilus Mensae region by McGill (2002) defined several geologic units that are similar to those described herein. The geologic history of this region included Middle Noachian and Hesperian resurfacing, Hesperian and Amazonian crater lakes, and formation of Hesperian to Amazonian smooth and lineated materials. Recent geologic mapping by Tanaka and others (2005) at 1:15,000,000 scale of the Martian northern plains have identified four material units that cover the map region: a widespread Noachian unit of continuous cratered highland plateau and large mesas, a Hesperian-Noachian unit of collapsed materials from basal sapping and mass wasting that forms part of the lowlands, and two Deuteronilus Mensae-specific units related to Hesperian and Amazonian deposition of ice-rich, mass-wasted debris.

DATA AND GIS MAPPING TECHNIQUES

Digital base maps, images, and ancillary information from the U.S. Geological Survey (USGS) were used in the geological mapping of the Deuteronilus Mensae region in conjunc-

tion with Geographic Information Systems (GIS) software. Datasets include a full-resolution (~50 m/pixel) Viking Orbiter Mars Transverse Mercator (MTM) base map, full-resolution (~50 m/pixel) Thermal Emission Imaging System (THEMIS) daytime Infrared (IR) and Visible (VIS) wavelength mosaics (data through 3/05), individual THEMIS IR and VIS images, 128 pixel/degree (~463 m/pixel) resolution Mars Orbital Laser Altimeter (MOLA) digital elevation model (DEM), gray and color synthetic hillshades of the MOLA DEM, and a 100-meter interval contour shapefile. The Viking base map is gap-free and covers the entire map region. Additional datasets used in our mapping and crater counts include a 256 pixel/degree (~231 m/pixel) resolution publicly released THEMIS daytime IR mosaic from Arizona State University (ASU), a 20 meters/pixel Mars Express High-Resolution Stereo Camera (HRSC) image, and individually processed Mars Orbiter Camera (MOC) narrow-angle images at resolutions higher than 12 meters/pixel. The THEMIS IR mosaic from ASU contains image data released subsequent to the USGS version, and covers the entire map region with ~17% data gaps. The HRSC image (h1483_0000_nd2.img) provided continuous coverage of the eastern half of the map region (~51%) and was used for crater counts. MOC images were used in selected areas to examine the surface morphology in detail.

The Viking, THEMIS, and MOLA DEM from USGS were all processed using Integrated Software for Imagers and Spectrometers (ISIS) software produced by the USGS Astrogeology Team. Map-projected THEMIS mosaics and images were produced from individual raw, radiometrically calibrated data. The HRSC data were processed using a modified version of the Video Image Communication And Retrieval (VICAR) software from the German Aerospace Center. All of the digital data, with the exception of HRSC and THEMIS IR from ASU, are in Transverse Mercator map projection with a center longitude of 30.0° E. and a center latitude of 0.0° using the International Astronomical Union (IAU) 2000 shape model of Mars (Seidelmann and others, 2002). For consistency, the HRSC and THEMIS IR from ASU were spatially adjusted in GIS to closely match the Transverse Mercator data.

Geologic units were mapped primarily on the Viking MTM base mosaic using Environmental Systems Research Institute (ESRI) ArcGIS ArcView software. Other mosaics or images were used where changes in image quality or lighting geometry occurred in the Viking mosaic. Contacts and structures were manually digitized and saved in an ArcGIS geodatabase for archiving and distribution. ArcGIS shapefiles exported from the geodatabase were later imported into Adobe Illustrator CS using a MAPublisher software plug-in. Relative age constraints for the geologic units were derived by counting the number and size distribution of superposed impact craters within the areas of each unit (for example, see Tanaka and others, 1992). The unit boundaries were digitized on Viking MTM and THEMIS daytime IR mosaics, and the surface area of each unit (polygon) was auto-calculated in ArcGIS. Impact craters were first counted using HRSC data covering the eastern half of the map region, followed by counts on the western half using Viking and THEMIS data. Although impact craters were more easily identified in the HRSC data due to its higher inherent resolution, craters down to 0.5 km in diameter could still be confidently identified in Viking and THEMIS data. Impact craters ,< 0.5 km in diameter were not counted. For all craters with a diameter > 0.5 km, the location, diameter (rim crest-to-crest), and image base used (Viking + THEMIS or HRSC) were recorded and saved in the geodatabase. Table 1 summarizes the size-frequency data for the cumulative number of craters > 2, 5, and 16 km in diameter normalized to 10^6 km^2. Figure 2 is a plot of the N(2) and N(5) crater data for all geologic units.

STRATIGRAPHY

Definitions of the geologic units are based on a combination of surface characteristics, contacts, and superposition relations in the image datasets that indicate differences in relative age. A total of eleven geologic units are defined and are divided into four groups: plateau material, plains material, impact crater material, and surficial material. Plateau material consists of the continuous ancient highland plateau and outcrops of the plateau in the form of polygonal mesas and small knobs scattered within the plains. Plains material consists of relatively flat expanses of smooth to hummocky deposits in low-lying areas north of the continuous highland margin. Impact crater material consists of rim, floor, and ejecta deposits of impact craters in a variety of preservation states, and Cerulli impact crater. Surficial material consists of lobate debris aprons and smooth fill deposits.

Relative age determinations for the geologic units are primarily based on observed superposition relations in the Viking and THEMIS mosaics, MOLA DEM, and crater densities for 2, 5, and 16 kilometer diameter craters (Tanaka, 1986; Tanaka and others, 1992). Several units have low numbers of superposed craters and their crater size-frequency data were not used in age designations. Figure 2 and table 1 show that N(2), N(5), and N(16) values for a given geologic unit do not always support designation of a single period or epoch because of differences in the number of craters in some size ranges relative to others. The complex geologic history of the region, including extensive erosion of ancient highland surfaces, has preferentially removed smaller craters on some surfaces. However, crater density data were generally useful in supplementing or refining observed relations to help constrain age ranges. In some cases, age designations were based strictly on observed superposition, cross-cutting, and contact relations of the geologic units (table 2). The locations of some of these relations, which are described in the following sections on material types, are shown in figure 3.

For consistency with an earlier geologic map by McGill (2002), which is adjacent to the eastern margin of this map, we used the primary and secondary attributes of surface materials in the identification and nomenclature of mapped units (for example, see Rotto and Tanaka, 1995). This resulted in defining units based on both stratigraphy and geomorphology/inferred erosional history. While this approach is different from planetary and terrestrial maps that follow a purely stratigraphic framework, it allows a visual representation of the overall geologic evolution similar to that shown by McGill (2002).

Plateau Material

Cratered highlands form most of the continuous plateau extending from the southern margin of the map region to the northern margin of Arabia Terra. Within the plateau and its remnants, three material units are identified. Lower smooth plateau material (unit Nplsl) consists of large flat mesa-like blocks north of the continuous plateau margin with top surface elevations ranging between –3,700 and –3,800 m. The blocks have low relief, generally no more than 100 m along their edges, with relatively featureless surfaces and sparse numbers of superposed craters. This material often underlies upper smooth plateau material to form layered polygonal mesas (lat 46.6° N., long 21.4° E.) that are topographically higher than adjacent smooth and mottled plains. This relation is clearly evident in Viking data and at local scales in THEMIS VIS images (fig. 4). The lower smooth plateau material unit forms parts of the Hesperian older channel and ridged plains units in the Mars eastern equatorial region geologic map by Greeley and Guest (1987), and unmapped, small outcrops of the widespread Noachian Noachis Terra unit within the local Amazonian Deuteronilus Mensae 2 unit in the northern plains geologic map by Tanaka and others (2005). The lower smooth plateau material unit is similar to the dark plateau unit mapped by McGill (2002).

North of the continuous plateau margin, upper smooth plateau material (unit Nplsu) occurs as high-standing polygonal mesas and smaller individual knobs or clusters of knobs within the northern lowlands. The top surfaces of mesas have a muted appearance compared to the plateau with low numbers of impact craters, most of which are less than a kilometer across in diameter. The steep mesa walls are smooth at Viking resolution, but in THEMIS VIS images, small alcoves are visible along the walls (fig. 5). Mesas have surface elevations ranging from –1,250 to –3,600 m that gradually decrease northward from the plateau margin. The mesas are topographically higher than the surrounding plains and surficial materials. A large high-standing circular mound at Deuteronilus Colles (lat 42.0° N., long 21.7° E.) includes irregular rounded knobs of smooth plateau materials. The knobs range in size from hundreds of meters to a few kilometers across. The mound lies at the center of a larger semi-circular area rimmed by polygonal mesas north of the continuous plateau margin (see fig. 1). The upper smooth plateau material unit is included as part of the highland terrain units in the Mars eastern equatorial region geologic map by Greeley and Guest (1987) and as part of the widespread Noachis Terra unit by Tanaka and others (2005). The upper smooth plateau material unit is similar to the smooth plateau unit mapped by McGill (2002).

South of the continuous plateau margin, upper smooth plateau material is characterized by a cratered surface with minor channels and large closed depressions. These surfaces have abundant primary impact craters up to a few tens of kilometers in diameter. Small sinuous channels, up to several kilometers long and a kilometer wide, cut parts of the plateau surface. The channels are not well developed and do not have prominent deposits at their termini. Several large closed depressions with irregular blocks or knobs of the plateau surface (fig. 6) are contained within a sub-circular basin in the plateau (lat 36.8° N., long 22.3° E.). The knobs and blocks range in size from a few hundred meters to several kilometers across. A few blocks have greater relief along one side of the block, suggesting that the top surface is tilted down into the surrounding smooth fill materials (fig. 7). Other blocks appear to expose at least two prominent layers along their margins (lat 36.6° N., long 23.2° E.). Much of the smooth plateau near the margin has been modified by the formation of fretted valleys (for example, Mamers Valles) and lobate debris aprons.

Dissected plateau material (unit Npld), found in association with upper smooth plateau material in the continuous highland plateau, exhibits surfaces that have been modified primarily by impact craters up to a few tens of kilometers in diameter and sinuous channels that are hundreds of meters to several tens of kilometers long and several hundred meters wide, similar to those in the upper smooth plateau materials. The number and apparent density of channels are much greater in this unit than in upper smooth plateau materials. The channels are concentric to the sub-circular basin (see fig. 6), and dissected plateau surfaces near the basin have gentle slopes (0.5–2.0° from MOLA data). The transition to adjacent upper smooth plateau material is often gradational and at the same relative elevation. Parts of the dissected plateau surface have been modified by secondary crater fields extending from Cerulli impact crater. The dissected plateau material unit forms part of the highland terrain units in the Mars eastern equatorial region geologic map by Greeley and Guest (1987) and part of the widespread Noachis Terra unit by Tanaka and others (2005). The dissected plateau material unit is similar to the hummocky plateau unit mapped by McGill (2002).

The three plateau material units represent the section of ancient highlands whose upper surfaces have been modified to various degrees by erosion and redistribution of material. The upper and lower smooth plateau materials together, form a layered sequence of the highlands. The dissected plateau material represents zones that have been influenced more by fluvial surface modification. The units themselves presumably consist of a combination of interbedded volcanic, sedimentary, and impact crater deposits.

Plains Material

North of the continuous plateau margin, most of the lowlands not covered by surficial materials consist of two plains units.

Smooth plains material (unit HNps) has relatively featureless surfaces that cover low-lying areas adjacent to plateau and impact crater materials. The smooth plains in turn, are covered in many locations by debris apron material. In some cases, small pockets of smooth plains are exposed where debris apron margins have either not fully converged or have receded (lat 44.8° N., long 24.0° E.). Where adjacent to mottled plains material, the elevations of the units are generally similar, with no embayment of mottled plains. A few isolated topographic lows within the smooth plains (lat 46.0° N., long 21.2° E.) have dark albedo surfaces in Viking MTM, MOC, and THEMIS VIS images compared to the rest of the plains (fig. 8). In MOC images, the

dark areas appear patchy, with wind streaks radiating out along their margins. Scattered clusters of small circular to irregular knobs (denoted by stipple pattern), with larger knobs mapped as upper smooth plateau material, are present in some portions of smooth plains material (lat 43.5° N., long 21.7° E.). Most of the smooth plains material is mapped as either Amazonian slide or Hesperian older channel materials in the Mars eastern equatorial region map by Greeley and Guest (1987) and as the early Hesperian Deuteronilus Mensae 1 unit by Tanaka and others (2005). The smooth plains material unit is similar to the smooth lowland plains unit mapped by McGill (2002).

Mottled plains material (unit Hpm) is topographically variable, consisting of bright flat-topped surfaces and lower dark hummocky surfaces in the Viking MTM base map (fig. 9). The margins of flat-topped surfaces are mostly bounded by low scarps, with an elevation difference of less than 100 m to the lower hummocky surface. The scarps are more apparent in low sun illuminated Viking images than in MOLA topography. Several resistant round knobs of upper smooth plateau material are scattered within the lower hummocky surface (lat 45.8° N., long 20.5° E.). The mottled plains have similar elevations to adjacent smooth plains materials, but are lower than upper and lower smooth plateau materials. This unit is not differentiated from the Hesperian older channel unit by Greeley and Guest (1987) or from the early Hesperian Deuteronilus Mensae 1 unit by Tanaka and others (2005) because of the differences in map scale. There is no single equivalent unit mapped by McGill (2002).

Plains materials include sedimentary deposits derived from erosion and local redistribution of the surrounding highlands and (or) from sources located in the northern lowland plains. Plains materials have accumulated in low-lying areas north of the continuous plateau margin. They consist of both smooth and mottled plains materials with the latter having a higher degree of topographic variability. Smooth plains materials may have been redistributed by flow, possibly facilitated by the incorporation of ice.

Impact Crater Material

Impact craters are a defining characteristic of the highland plateau (Tanaka and others, 2005), and where ejecta blankets and (or) crater rim materials are well defined, they are mapped as distinct units. Much of the southern portion of the map is covered by ejecta related to Cerulli impact crater. Other impact crater materials are located primarily in the continuous plateau, with lesser numbers in the lowland plains. There are numerous rimless craters throughout the older plateau materials (units Npld, Nplsu, Nplsl) that are part of the overall degradational signature of these units, but not mapped as individual crater material units. Three types of crater materials are identified based on their preservation state. Only impact craters with diameters greater than 3 km have been mapped.

Cerulli crater material (unit Ncc) is characterized by a continuous ejecta blanket and a pronounced, continuous rim (diameter = 125 km) that is elevated relative to the surrounding surfaces. Numerous channels cut the interior walls of the crater (lat 32.8° N., long 22.1° E.) and the outer portions of the ejecta blanket. The ejecta deposits are moderately preserved, and the floors of numerous low-lying flats in and around the crater rim are covered with smooth fill material. Secondary craters and crater fields are scattered throughout the ejecta blanket and extend onto other geologic units. Several linear grooves are radial to the crater center.

Highly degraded crater material (unit c_1) is characterized by a partial to discontinuous rim with little or no relief relative to the surrounding surfaces or ejecta blanket (if present). These are significantly modified deposits that form the ejecta, rims, and floors of impact craters. The ejecta of a few craters could only be identified from brightness differences in THEMIS daytime IR data (lat 42.7° N., long 21.0° E.). The crater floors are often partially or entirely covered by smooth fill or debris apron materials. Moderately degraded crater material (unit c_2) is characterized by a continuous rim with minor relief relative to the surrounding surfaces and a continuous to semi-continuous ejecta blanket. These deposits form the ejecta, rims, and floors of impact craters. The deposits generally have smooth to pitted surfaces. Well-preserved crater material (unit c_3) is characterized by a pronounced, continuous rim with significant relief relative to the surrounding surfaces and a continuous ejecta blanket. These crater materials exhibit little degradation and form the ejecta, rims, and floors of fresh impact craters. Some ejecta lobes have rampart margins (lat 42.4° N., long 22.4° E.) that range from thin, tongue-like flow lobes that extend from the hummocky outer rim area to larger circular lobate flow lobes with escarpment terminations and lineated grooves that extend radially from below the rim crest.

Surficial Material

Surficial material generally covers all plateau and plains materials in the map area. Two material units are identified.

Debris apron material (unit Ada) occurs as smooth lobate deposits with gentle surface slopes (0.4°–8.0° from MOLA data) that surround and extend beyond the bases of mesas, knobs, crater rims, and fretted valley walls. Debris apron surfaces have lineations parallel or transverse to apparent flow direction. Deposits near the base of the slope are sometimes partially covered by one or more apron deposits from above, forming successive lobate fronts. Near the plateau margin (lat 39.8° N., long 23.0° E.), bulbous lobes extend through breaks in the plateau materials (fig. 10). Several of the lobes have margins that are deflected around obstacles such as blocks of upper smooth plateau material (fig. 11). Along the margins of the mound at Deuteronilus Colles, THEMIS IR and VIS images show at least one lobe that has flowed onto the adjacent smooth plains (fig. 12). Apron materials often embay other units such as impact crater, plains, and plateau materials. In a few cases, portions of the apron margin have ridges of apron material, forming a ribbed appearance (fig. 13, denoted by stipple pattern). At the bases of some knobs and fretted valleys, a 1- to 2-km-wide gap is apparent between the slope base and the head of the debris apron. This unit forms part of the Amazonian slide materials in the Mars eastern equatorial region map by Greeley and Guest (1987) and part of the Deuteronilus Mensae 2 unit by Tanaka

and others (2005). Debris apron material is most similar to and consistent with debris apron materials mapped by McGill (2002).

Smooth fill material (unit Afs) occurs as deposits with relatively featureless surfaces that cover low-lying areas below scarps, between plateau blocks in collapse depressions, at the margins of some fretted valleys adjacent to plateau materials, and on the floors of many impact craters. The floor of Cerulli impact crater, as well as small local flats along its rim, exhibit smooth fill material. The margins of smooth fill materials do not have relief or lobate forms. The largest craters with fill material, excluding Cerulli, have concentric grooves that follow the shape of the crater walls (lat 36.8° N., long 22.3° E.). Some collapse depression floors have patches of small knobs (not individually mapped, but denoted by stipple pattern) scattered within the smooth fill, producing a hummocky appearance (see fig. 6). The smooth fill materials are local deposits that are not mappable at the scale of the Mars eastern equatorial region geologic map by Greeley and Guest (1987) and the northern plains geologic map by Tanaka and others (2005). The smooth fill material unit is most similar to the older and younger smooth plains units mapped by McGill (2002).

Overall, surficial materials represent the most recent phase of erosion and deposition in the map region. These are sediments that accumulated in local low-lying regions and are derived from remnants of the ancient highland plateau, impact crater materials, and younger plains units. Smooth fill and debris apron materials are likely composed of talus and debris shed from adjacent hillslopes mixed with eolian deposits that cover the surfaces of older exposed units. Debris aprons have clear indications of flow in the form of bulbous lobes, flow lineations, and deflection around obstacles. Flow of debris apron materials is likely facilitated by the incorporation of ice. In high resolution MOC images, debris aprons and some smooth fill surfaces appear to be covered by mantle deposits that exhibit a variety of textures.

STRUCTURAL FEATURES

Several morphologic features provide both direct and indirect evidence for tectonic activity in the map region. These features include wrinkle ridges, grabens, and closed depressions. Wrinkle ridges and grabens are not abundant, and are located primarily in the ancient highland plateau (Lucchitta, 1976, 1977; Chicarro and others, 1985; Plescia and Golombek, 1986; Watters, 1988, 1991, 1993; Zuber, 1995). Most ridge axes are linear, but some are curved along their lengths. Grabens in the map area are generally short, narrow linear depressions, not the wide prominent forms typically found in regions such as Coloe Fossae and Nili Fossae. The closed depressions are large features that may have initially formed by collapse of an unstable surface but have widened over time through erosion and mass wasting along their margins. Disruption and modification of the continuous plateau from tectonic activity early in the history of Mars may have led to the development of fracture lanes (McGill, 2002), which isolated portions of the plateau, leading to the formation of polygonal mesas. The presence of these structural features indicates that plateau materials in the Deuteronilus Mensae region have been modified by surface instability and deformation, along with subsidence and collapse (see discussion section).

DISCUSSION

Plateau Modification and Closed Depressions

Within upper smooth plateau material, three prominent large, elongate, closed depressions 300–500 m deep contain numerous polygonal blocks and rounded knobs (lat 35.7°–37.7° N., long 21.0°–23.6° E., see fig. 6). The blocks do not appear to be rotated but some have sloped upper surfaces dipping in toward the depression floor suggesting that they have been tilted. The top surfaces of some blocks are at an elevation that is similar to, or higher than, the surfaces surrounding the depressions, which indicates that parts of the original surface surrounding the blocks have subsided or collapsed. We interpret the blocks and knobs to be in-situ remnants of plateau materials that have further subsided and been eroded over time. The blocks or knobs have different sizes and abundances, indicating different states of highland modification.

A fundamental issue regarding the origin of the depressions is removal of subsurface support that allowed subsidence and collapse to occur. Their lack of apparent outlets, either along the depression margins or surface channels outside of the depressions, suggests that material was not likely removed by fluvial processes. Winds have the ability to remove and (or) redistribute some surface materials; however, a growing surface depression may also trap eolian deposits. It is unclear that wind alone could remove hundreds of cubic kilometers of material to form these depressions. If volatiles were present in plateau materials, then sublimation of ice could remove some of the total volume from near the surface, but it is unclear how much of this ice was interstitial or what fraction could become trapped at depths far below the surface.

The loss of material could be related to volatile-rich zones at depth that were once, or still are, present in the plateau. The development of fractures and (or) release of volatiles could have been initiated by a variety of processes. Solution collapse where soluble rock below an insoluble layer undergoes dissolution by the passage of groundwater is a possibility. This process is difficult to assess due to the lack of discharge areas near the depressions that would indicate subsurface water migration, lack of evidence for exposed diagnostic minerals such as carbonates from THEMIS IR data, and mantling of the surface by eolian deposits and other mass-wasted fill materials. Buried subsurface heterogeneities (for example, sedimentary layers with different permeabilities, faults, and impact craters, see [Malin and Edgett, 2001] or [Edgett and Malin, 2002]) may have created volatile-rich lenses or zones. If these volatiles were mobilized, then they could have destabilized the overlying materials, resulting in fracturing and subsidence or collapse of the surface. The rise and intrusion of magma bodies such as volcanic sills or dikes

could have mobilized volatiles in the subsurface. Although there is no clear surface expression of exposed intrusive bodies in the plateau, their existence at depth cannot be ruled out. Another possible contributor to the disruption, fracturing, and movement of subsurface materials are large impacts (Newsom, 1980; Melosh, 1989; Clifford, 1993; Williams and Greeley, 1994). Ground shaking from the seismic energy released by an impact is likely to have disrupted the subsurface plateau materials, producing fractures that could grow, leading to subsidence and (or) collapse. Overall, subsidence and (or) collapse has played an important early role in the modification of this region and other regions of Mars (McCauley and others, 1972; Sharp, 1973b; Schonfeld, 1979; Nummedal and Prior, 1981; Tanaka and Golombek, 1989; Davis and Golombek, 1990; Crown, 2005; Rodriguez and others, 2005, 2006).

Assessment of Potential Lowland Water Bodies

The existence of a large ocean, or oceans, covering the northern lowlands of Mars was first proposed by Parker and others (1989, 1993) on the basis of geomorphic features in Viking Orbiter images attributed to coastal processes. The putative ocean was thought to be present during the Noachian Period and as late as the Early Amazonian Epoch. This hypothesis has recently been reevaluated using hydrological models, climate models, and from a variety of new datasets beginning with the Mars Global Surveyor (MGS) mission (Head and others, 1999; Malin and Edgett, 1999; Thomson and Head, 1999; Clifford and Parker, 2001; McGill, 2001; Carr, 2001; Withers and Neumann, 2001; Kreslavsky and Head, 2002; Fairen and others, 2003; Carr and Head, 2003; Webb, 2004; Ghatan and Zimbelman, 2006; Perron and others, 2007). Results from these studies have been mixed, some of which support a large body of water, but most requiring further investigation due to insufficient evidence or alternative process(es) that could produce similar geomorphic features.

Malin and Edgett (1999) describe in detail the geomorphic features and textural changes that should be present if an ocean or other persistent body of water once existed and retreated on the surface. Geomorphic features include beach ridges, bars, spits, wave-cut terraces or platforms, and fluviolacustrine deltas. Textural changes could include the presence of clays or other fines or the formation of evaporite minerals. Horizontally bedded sediments or layers such as hyaloclastic tuffs, maars, or other constructs from underwater volcanic eruptions would also be an indicator that a former ocean or lake was present.

Our analysis of Viking, THEMIS, MOC, and MOLA data in the map region did not yield diagnostic geomorphic features such as flat benches, ridges, or other topographic signatures along plateau escarpments or mesa walls where a shoreline would be expected. Older Noachian to Hesperian surfaces along the dichotomy boundary and in the lowlands are mostly covered by large expanses of debris apron material, making it difficult to find such changes along a potential shoreline (Tanaka and others, 2003, 2005). Resistant rock outcrops with consistent elevation levels are present along some escarpments and mesa walls, but many are discontinuous in places, and these outcrops may be related to different material layers rather than indications of past sea-level stands. Consistent changes in albedo or surface roughness were also not observed. The entire Deuteronilus Mensae map region is located within the Contact 1 (Parker and others, 1989, 1993) or Arabia shoreline area (fig. 1) as defined by Clifford and Parker (2001).

The lack of distinct geomorphic features related to coastal activity does not preclude the hypothesis that an ocean or other former standing bodies of water were once present along the continuous plateau margin (Scott and others, 1995). One of the challenging issues with identifying such features is their preservation over billions of years. If these features were formed as early as the Noachian Period, it is unlikely they would remain identifiable due to erosion and redistribution of materials. If the Arabia shoreline or any others were previously present in this region, they would pre-date the young resurfacing that has occurred (debris aprons and surficial fill). Erosion of the escarpment and the formation of lobate debris aprons would have caused plateau retreat and altered possible topographic evidence of relict features related to coastal processes.

GEOLOGIC HISTORY

The following description of the geologic history is based on photogeologic interpretation of the landforms and surfaces observed in combination with age constraints from crater size-frequency data.

Noachian Period

During the Noachian Period, the highland plateau, likely volcanic and sedimentary materials reworked by impacts (Tanaka and others, 2005), may have once covered much of the plains north of the current continuous plateau margin, but has been modified since by tectonics, impacts, and surface fluid flow. The current-day polygonal mesas and linear segments of fretted valleys suggest that tectonic activity (Banerdt and others, 1992), perhaps related to formation of the dichotomy boundary (see Watters and McGovern, 2006 and references therein), may have produced fracture lanes (McGill, 2002) and facilitated development of a structural fabric with roughly orthogonal cracks or joints in upper and lower smooth plateau, and dissected plateau materials (Kochel and Peake, 1984). To what depth this fabric extends is unknown, but where tectonic activity (or impact cratering) caused breakup of the crust, these sites would have been candidates for widening along cracks, faults, or other subsurface discontinuities by erosion. The modification and isolation of plateau materials by tectonic and (or) impact cratering during the Noachian Period likely influenced the later development of polygonal mesas in the Deuteronilus Mensae region.

Tectonic activity may have also played a role in tilting the plateau materials such that they gently slope down into the present-day lowland plains north of the continuous plateau margin (McGill, 2000, 2001). A north-dipping slope is consistent with the decreasing surface elevations of individual mesa tops in

MOLA data. Further analyses of the topography from the continuous plateau to the northern extent of polygonal mesas show similar elevations for near-boundary mesas and the continuous highlands, but differences in the elevations of far-boundary mesas (fig. 14). These differences, along with the general decrease in impact craters northward of the continuous plateau, could be attributed to an erosional event that removed the upper portion of upper smooth plateau materials, similar to the Noachian resurfacing identified by McGill (2002). This major resurfacing event is difficult to assess in the map region due to the Hesperian and Amazonian resurfacing that has modified and covered much of the older Noachian units. Alternatively, the difference may be related to the general decrease in plateau elevation towards the north (slopes down into the lowlands). A clear stratigraphic relation exists between upper and lower smooth plateau materials; upper smooth plateau material consistently overlies lower smooth plateau material. This sequence and their shared contacts suggest that lower smooth plateau surfaces may be exposed lower layers of plateau materials. Surface erosion of the ancient highland plateau likely occurred during the Late Noachian to possibly Early Hesperian Epoch, prior to the formation of fretted valleys, polygonal mesas, and collapse depressions.

Coeval with regional tectonic activity are impact events that formed craters and basins now preserved as semi-circular structures rimmed by plateau material. The mound of small rounded knobs at Deuteronilus Colles may be the central peak of one of these impact structures. These features may have been buried at various depths within the ancient plateau (Edgett and Malin, 2002), and their presence could have influenced the subsequent erosional patterns of highland materials. Sediments (and perhaps volatiles) trapped within these structures may have been more easily subjected to collapse and erosion relative to rim materials, thus forming the semi-circular structures exposed on the surface today. These ancient structures and smaller impacts, in combination with tectonic activity, likely caused further disruption and fracturing of subsurface materials to form megaregolith (Clifford, 1981), creating an environment that facilitated the migration of fluids within the subsurface and to the surface. These fluids may have been sufficient to cause minor fluvial dissection, producing the dissected plateau materials. Alternatively, the fluids may be related to periods of sustained flow from surface runoff by precipitation or other sources (McCauley and others, 1972; Sharp and Malin, 1975; Baker, 1982; Baker and others, 1992; Carr 1996). Observations that surface dissection is not widespread and mostly confined to dissected plateau surfaces suggest a subsurface source and (or) efficient infiltration through unconsolidated surface materials with reemergence and dissection in select localities.

Cerulli impact crater has numerous channels along its interior walls and within its ejecta blanket. These channels indicate post-impact surface fluid flow (Mouginis-Mark, 1987). The presence of flow lobes within the ejecta blanket (Melosh, 1989) provides additional evidence that plateau materials may have been volatile-charged during the Noachian and on into the Hesperian Period. Although impact melt could also produce similar channels (Howard and Wilshire, 1975) and atmospheric effects on the impact ejecta curtain could produce multi-lobed patterns (Schultz and Gault, 1979), the preferred explanation is the presence of subsurface volatiles (Mouginis-Mark, 1987; Melosh, 1989). There is uncertainty about the specific timing of the Cerulli impact event but based on the N(5) crater density value, it was likely Middle to Late Noachian.

Hesperian Period

The formation of laterally and vertically heterogeneous highland terrain and the disruption and fracturing of the plateau from tectonic and impact processes in the Noachian Period likely created conditions for subsidence and (or) surface collapse, as evidenced by the closed depressions with in-situ blocks of upper smooth plateau material. Although there are no morphological features that indicate fluid flow exiting the depressions, subsurface fluid migration and possible dissolution (see discussion section) could have been a contributing factor to loss of support and subsequent collapse or subsidence of the overlying plateau (Chuang and Crown, 2007). Continued erosion of the collapse depressions caused widening of their margins, infilling of mass-wasted wall materials, and an overall transition from polygonal blocks to smaller remnant rounded knobs, producing hummocky floors. McGill (2002) noted the presence of former lakes within old impact craters during the Hesperian Period. However, similar to the lack of observed inlets or outlets for the collapse depressions, the lack of crater-intersecting inlet valleys or channels indicates that fluvial activity related to lacustrine environments may have been more well developed or persistent east of this map area.

Breakup and erosion of the plateau, particularly north of the present-day continuous margin, further isolated portions of smooth plateau materials, causing gradual retreat of block margins that reduced their size, producing the isolated blocks and clusters of polygonal mesas now present in the lowlands. This activity may have also modified individual crater forms and basins. Erosion likely involved both physical and chemical weathering of plateau materials including ice sublimation and melting, cracking from thermal expansion and contraction, wind abrasion, and other processes such as mass wasting. Talus deposits along block margins may have incorporated ice from water vapor that diffused into the soil and froze when Mars had a thicker atmosphere (Clifford and Hillel, 1983; Clifford, 1993; Mellon and Jakosky, 1993; Carr, 1996) and (or) been covered by ancient ice-rich mantling deposits in a manner similar to that postulated for recent Martian climate regimes (Mustard and others, 2001; Milliken and others, 2003; Christensen, 2003). Redistribution of these deposits may have occurred by ice creep processes (Squyres, 1978, 1979; Lucchitta, 1984; Squyres and Carr, 1986) or by mass flows facilitated by ice-rich interior zones (Baker, 2001). In addition, ice lenses buried at depth in the highland plateau may have facilitated failure and mass wasting of plateau materials. The coalescence and flow of these deposits, along with mantling and reworking of eolian materials likely formed the smooth plains. This activity is likely an older stage of ice-rich flow that may be similar to the younger debris aprons observed in the region. Some isolated areas have smaller rounded knobs within the smooth plains. The knobs may be

remnant blocks of upper smooth plateau materials that have not been completely eroded. In the area east of this map region, McGill (2002) suggested that an erosional event that formed the fretted valleys and terrain may have been a result of sapping and surface-water flow. Although these processes are plausible for this map region, the evidence of collapse structures suggests that development of fretted valleys may have been facilitated by the widening of pits and (or) cracks along the margin of the continuous plateau due to erosion and mass wasting. The preserved elongate collapse depressions within a remnant highland basin in the map region may represent an initial stage of plateau breakup, with continued collapse-dominated phases leading to formation of fretted terrain valleys and mesas. The eventual formation of polygonal mesas and knobs at the expense of mass-wasted plateau materials is consistent with a previous study of the Deuteronilus Mensae region by Kochel and Peake (1984).

In the northernmost portion of the map region, areas where upper and lower smooth plateau materials are not present, topographically variable materials form the uneven mottled plains. The origin of the mottled plains is unknown but their formation could be related to further erosion and redistribution of highland plateau units, a transition from the cratered highlands to the northern lowlands (for example, the mottled plains includes sedimentary deposits with sources in the lowlands), or bright patches of Lyot crater ejecta deposits on top of smooth dark fill materials that have not been covered by smooth plains or other younger surficial materials. These bright patches are within 120 km of the observed margin of the continuous ejecta blanket of Lyot crater (diameter = 215 km). The formation and redistribution of plains materials likely ended late in this period with most of the lowlands covered by smooth or mottled plains materials.

Amazonian Period

Ice-driven resurfacing along the margins of polygonal mesas, knobs, and fretted valleys, along with infilling of debris in low-lying areas, played a dominant role during this time period. Smooth fill materials cover the floors of closed depressions, the margins of some fretted valleys adjacent to plateau materials, impact craters including Cerulli crater, and the small low-lying flats along the rim of Cerulli crater. Within closed depressions, smooth fill materials are likely talus and blocks of eroded wall materials mixed with some eolian deposits; within impact craters, the smooth fill materials are likely a combination of eolian, mass-wasted, and (or) fluvial deposits mixed with possible impact melt or impact brecciated rocks that cover the crater floor. In a few of the well-preserved impact craters, concentric ridges form a pattern of grooved fill. The formation of these ridges is likely from the interaction of convergent flows of ice-rich materials toward the crater center (Squyres, 1978; 1979). Alternatively, the ridges could be remnants of eroded air-fall deposits that exhibit similar morphologies (Zimbelman and others, 1989). Deposition of smooth fill materials likely occurred to different extents at different times and in different locations throughout the map region; deposition of smooth fill is assumed to be Amazonian and may have continued into the Late Amazonian Epoch.

Lobate debris aprons surround and extend beyond the bases of mesas, knobs, crater rims, and fretted valley walls. In most cases, multiple apron lobes have converged to form a single apron mass (see Pierce and Crown, 2003) that spreads over plains and impact crater materials. The surface lineations, convex-up margins (see cross section *A–A'* in fig. 14), and deflection of apron margins around obstacles indicate downslope flow of material. Lobate debris aprons have been interpreted and modeled as a variety of possible features including rock glaciers, ice-rich mass movements, or debris-covered glacial flows (Lucchitta, 1984; Baker, 1991; Colaprete and Jakosky, 1998; Baker, 2001; Mangold and Allemand, 2001; Crown and others, 2002, 2003, 2006; Mangold, 2003; Pierce and Crown, 2003; Turtle and others, 2003; Head and others, 2005; Li and others, 2005; Chuang and Crown, 2005a,b,c, 2006). However, it is unclear what abundance and distribution of ice exists within the aprons, and whether the source of the ice was from the ground (related to the ancient Martian cryosphere [Carr, 1996]) or from recent periods of cold climate due to obliquity-driven changes (Laskar and Robutel, 1993; Touma and Wisdom, 1993; Head and others, 2003). Recent studies of localized mantle deposits within the source areas of gullies suggest that snowpacks could also be a possible source of ice even under current-day conditions (Christensen, 2003). The abundance of debris aprons throughout this map region is consistent and in agreement with debris aprons mapped by McGill (2002), which indicates that ice-rich movement of debris has occurred over a significant period of Martian history and that debris aprons are older than the mantle deposits.

In many locales near the bases of knobs and fretted valleys (lat 40.1° N., long 23.6° E. and lat 45.8° N., long 23.1° E.), a gap up to 2 km wide is apparent between the base of the hillslope and the head of the debris apron (see fig. 5). This gap may represent an area where the upper apron margin has retreated or a period in which the apron mass has advanced downslope, but with a cutoff in supply. Similar gaps, described as moats, are observed in MOLA profiles of lobate debris aprons in eastern Hellas (Pierce and Crown, 2003). The successive lobate fronts of debris aprons near the continuous plateau margin suggests that major apron forming events may be episodic. Although there is a lack of evidence for current downslope flow of individual aprons, the positions of terminal margins where multiple fronts are observed along a slope are similar, indicating movement as a single coherent mass even though individual lobes may form due to obstacles at the front. Thus, at least two apron-forming events are apparent, and they suggest periods of sustained debris supply from mass wasting and incorporation of ice to facilitate flow of materials. The occurrence of a ribbed pattern of ridges along some apron fronts suggests that either partial retreat of the apron margin or apron deposition over an uneven pre-existing surface (see fig. 13) may have produced the ribbed appearance. In terms of partial retreat, the ridges may be accumulations of basally scoured and (or) talus materials that now mark the former extent(s) of the aprons (Hauber and others, 2008).

Debris-apron surfaces within a network of theater-headed alcoves and cirque-like accumulation zones in a T-shaped fretted valley (lat 37.7° N., long 24.0° E.) near the eastern edge of

the mapping region suggest that some debris aprons are analogous to terrestrial valley glaciers (Head and others, 2006b). The aprons were observed to have parallel, converging, chevron-like flow lineations, convergent fold structures, and flow constriction through narrow valley passages. Head and others (2006b) suggested that these are well-preserved features of past glacial ice flow and that significant climate change must have occurred during the Late Amazonian Epoch to cause sustained snow and ice accumulation to feed the valley glaciers. They also suggest that, if debris aprons are analogous to terrestrial glaciers, then sublimation till may have protected the surface and kept ice cores intact up to the present time. Although the similarity in surface morphology is striking, most debris aprons in the map region do not share these same characteristics. This suggests that either the conditions for glacial flow were somehow confined to this fretted valley or that preservation of glacial flow features is relatively poor for debris aprons in this region.

Contemporaneous with or subsequent to the growing extent of debris aprons was the deposition and partial removal of mantle deposits on debris apron, polygonal mesa, plains, and plateau surfaces. A variety of surface textures, particularly on debris aprons, indicate the presence of these mantle deposits, including smooth surfaces with minor pitting, knobby, lineated, and an undulating ridge-and-valley surface (Mangold, 2003; Pierce and Crown, 2003). These textures at THEMIS VIS scale are common on most debris aprons in the map region and are likely formed within a layer of ice-cemented dust or other fines (fig. 15). Sublimation of ice in the mantle deposit may have liberated the dusty material, which is subsequently redistributed by eolian processes. Overall, the mantle deposits appear to be similar to the mantling deposits prominent throughout the mid-latitudes of Mars (Carr, 2001; Mustard and others, 2001; Mangold, 2003; Pierce and Crown, 2003; Milliken and others, 2003; Chuang and Crown, 2005a).

ACKNOWLEDGMENTS

We appreciate the thorough and constructive comments by James Skinner and George McGill, which improved the quality of this map. We thank Bob Sucharski at the U.S. Geological Survey for generating the digital base maps and other GIS data for our map work. This report is based upon work supported by the National Aeronautics and Space Administration under Grant No. NNG04GI85G issued through the Planetary Geology and Geophysics Program. This map is PSI Contribution 447.

REFERENCES CITED

Andrews-Hanna, J.C., Zuber, M.T., and Banerdt, W.B., 2008, The Borealis basin and the origin of the Martian crustal dichotomy: Nature, v. 453, p. 1212–1215.

Baker, V.R., 1982, The channels of Mars: Austin, Tex., University of Texas Press, 204 p.

Baker, V.R., 1991, Ancient oceans, ice sheets and the hydrological cycle on Mars: Nature, v. 352, p. 589–594.

Baker, V.R., 2001, Water and the Martian landscape: Nature, v. 412, p. 228–236.

Baker, V.R., Carr, M.H., Gulick, V.C., Williams, C.R., and Marley, M.S., 1992, Channels and valley networks, *in* Kiefer, H.H., Jakosky, B.M., Snyder, C.W., and Mathews, M.S., eds., Mars: Tucson, Ariz., University of Arizona Press, p. 493–522.

Banerdt, W.B., Golombek, M.P., and Tanaka, K.L., 1992, Stress and tectonics on Mars, *in* Kiefer, H.H., Jakosky, B.M., Snyder, C.W., and Mathews, M.S., eds., Mars: Tucson, Ariz., University of Arizona Press, p. 249–297.

Carr, M.H., 1996, Water on Mars: New York, Oxford University Press, 229 p.

Carr, M.H., 2001, Mars Global Surveyor observations of Martian fretted terrain: Journal of Geophysical Research, v. 106, p. 23,571–23,593.

Carr, M.H., and Head, J.W. III, 2003, Oceans on Mars—An assessment of the observational evidence and possible fate: Journal of Geophysical Research, v. 108, no. E5, p. 8-1 to 8-28 (doi:10.1029/2002JE001963).

Chicarro, A.F., Schultz, P.H., and Masson, P., 1985, Global and regional ridge patterns on Mars: Icarus, v. 63, p. 153–174.

Christensen, P.R., 2003, Formation of recent Martian gullies through melting of extensive water-rich snow deposits: Nature, v. 422, p. 45–48.

Chuang, F.C., and Crown, D.A., 2005a, Surface characteristics and degradational history of debris aprons in theTempe Terra/Mareotis Fossae region of Mars: Icarus, v. 179, p. 24–42.

Chuang, F.C., and Crown, D.A., 2005b, Martian debris aprons—Morphometric comparisons of the eastern Hellas and Tempe/Mareotis populations [abs.]: Houston, Tex., Lunar and Planetary Institute, Lunar and Planetary Science Conference, XXXVI, Abstract no. 1519 [CD-ROM].

Chuang, F.C., and Crown, D.A., 2005c, Geomorphic analyses of lobate debris aprons in Deuteronilus Mensae, Mars: EOS Transactions, v. 86, no. 52, American Geophysical Union Fall Meeting Supplement, no. P23A-0176.

Chuang, F.C., and Crown, D.A., 2006, Corrigendum to "Surface characteristics and degradational history of debris aprons in the Tempe Terra/Mareotis Fossae region of Mars" (Icarus 179 (2005) 24-42): Icarus, v. 181, p. 623–624.

Chuang, F.C., and Crown, D.A., 2007, Modification of the ancient highland plateau along the Dichotomy Boundary, Deuteronilus Mensae, Mars [abs.]: Houston, Tex., Lunar and Planetary Institute, Lunar and Planetary Science Conference, XXXVII, Abstract no. 1455 [CD-ROM].

Clifford, S.M., 1981, A pore volume estimate of the Martian megaregolith based on a lunar analog [abs.]: International Colloquium on Mars, 3rd, Pasadena, California, Aug. 31–Sept.2, Lunar and Planetary Institute, contribution no. 441, p. 46–48.

Clifford, S.M., 1993, A model for the hydrologic and climatic behavior of water on Mars: Journal of Geophysical Research, v. 98, p. 10,973–11,016.

Clifford, S.M., and Hillel, D., 1983, The stability of ground ice in the equatorial regions of Mars: Journal of Geophysical Research, v. 88, p. 2456–2474.

Clifford, S.M., and Parker, T.J., 2001, The evolution of the Martian hydrosphere—Implications for the fate of a primordial ocean and the current state of the northern plains: Icarus, v. 154, p. 40–79.

Colaprete, A., and Jakosky, B.M., 1998, Ice flow and rock glaciers on Mars: Journal of Geophysical Research, v. 103, no. E3, p. 5897–5909.

Crown, D.A., 2005, Styles and timing of volatile-driven activity in the eastern Hellas region of Mars: Journal of Geophysical Research, v. 110, no. E12S22, p. 1–19 (doi: 10.1029/2005JE002496).

Crown, D.A., Chuang, F.C., Berman, D.C., and Miyamoto, H., 2006, Ice-driven degradation styles in the Martian mid-latitudes: Constraints from lobate debris aprons, lineated valley fill, and small flow lobes [abs.]: Houston, Tex., Lunar and Planetary Institute, Lunar and Planetary Science Conference, XXXVII, Abstract no. 1861 [CD-ROM].

Crown, D.A., McElfresh, S.B.Z., Pierce, T.L., and Mest, S.C., 2003, Geomorphology of debris aprons in the eastern Hellas region of Mars [abs.]: Houston, Tex., Lunar and Planetary Institute, Lunar and Planetary Science Conference, XXXIV, Abstract no. 1126 [CD-ROM].

Crown, D.A., Pierce, T.L., McElfresh, S.B.Z., and Mest, S.C., 2002, Debris aprons in the eastern Hellas region of Mars: Implications for styles and rates of highland degradation [abs.]: Houston, Tex., Lunar and Planetary Institute, Lunar and Planetary Science Conference, XXXIII, Abstract no. 1642 [CD-ROM].

Davis, P.A., and Golombek, M.P., 1990, Discontinuities in the shallow Martian crust [abs.]: Houston, Tex., Lunar and Planetary Institute, Lunar and Planetary Science Conference, XX, p. 224–225.

Edgett, K.S., and Malin, M.C., 2002, Martian sedimentary rock stratigraphy— Outcrops and interbedded craters of northwest Sinus Meridiani and southwest Arabia Terra: Geophysical Research Letters, v. 29, no. 24, p. 32-1 to 32-4 (doi:10.1029/2002GL016515).

Edgett, K.S., and Parker, T.J., 1997, Water on early Mars—Possible subaqueous sedimentary deposits covering ancient cratered terrain in western Arabia and Sinus Meridiani: Geophysical Research Letters, v. 24, p. 2897–2900.

Fairen, A.G., Dohm, J.M., Baker, V.R., de Pablo, M.A., Ruiz, J., Ferris, J.C., and Anderson, R.C., 2003, Episodic flood inundations of the northern plains of Mars: Icarus, v. 165, p. 53–67.

Frey, H.V., 2006, Impact constraints on the age and origin of the lowlands of Mars: Geophysical Research Letters, v. 33, no. L08S02, p.1–4 (doi:10.1029/2005GL024484).

Frey, H.V., and Schultz, R.A., 1988, Large impact basins and the mega-impact origin for the crustal dichotomy on Mars: Geophysical Research Letters, v. 15, p. 229–232.

Ghatan, G.J., and Zimbelman, J.R., 2006, Paucity of candidate coastal constructional landforms along proposed shorelines on Mars—Implications for a northern lowlands-filling ocean: Icarus, v. 185, p. 171–196.

Greeley, R., and Guest, J.E., 1987, Geologic map of the eastern equatorial region of Mars: U.S. Geological Survey Miscellaneous Investigations Series Map I–1802B, scale 1:15,000,000.

Hauber, E., Van Gasselt, S., Chapman, M.G., and Neukum, G., 2008, Geomorphic evidence for fomer lobate debris aprons at low latitudes on Mars—Indicators of the Martian paleoclimate: Journal of Geophysical Research, v. 113, no. E02007, p. 1–11 (doi:10.1029/2007JE002897).

Head, J.W., III, Hiesinger, H., Ivanov, M.A., Kreslavsky, M.A., Pratt, S., and Thomson, B.J., 1999, Possible ancient oceans on Mars—Evidence from Mars Orbiter Laser Altimeter: Science, v. 286, p. 2134–2137.

Head, J.W., Marchant, D.R., Agnew, M.C., Fassett, C.I., and Kreslavsky, M.A., 2006b, Extensive valley glacier deposits in the northern mid-latitudes of Mars—Evidence for Late Amazonian obliquity-driven climate change: Earth and Planetary Science Letters, v. 241, p. 663–671.

Head, J.W., Mustard, J.F., Kreslavsky, M.A., Milliken, R.E., and Marchant, D.R., 2003, Recent ice ages on Mars: Nature, v. 426, p. 797–802.

Head, J.W., Nahm, A.L., Marchant, D.R., and Neukum, G., 2006a, Modification of the dichotomy boundary on Mars by Amazonian mid-latitude regional glaciation: Geophysical Research Letters, v. 33, no. L08S03, p. 1–3 (doi:10.1029/2005GL024360).

Head, J.W., Neukum. G., Jaumann, R., Hiesinger, H., Hauber, E., Carr, M., Masson, P., Foing, B., Hoffmann, H., Kreslavsky, M., Werner, S., Milkovich, S., van Gasselt, S., and the HRSC Co-Investigator Team, 2005—Tropical to mid-latitude snow and ice accumulation, flow and glaciation on Mars: Nature, v. 434, p. 346–351.

Howard, K.A., and Wilshire, H.G., 1975, Flows of impact melt at lunar craters: Journal of Geophysical Research, v. 3, p. 237–251.

Irwin, R.P., Watters, T.R., Howard, A.D., and Zimbelman, J.R., 2004, Sedimentary resurfacing and fretted terrain development along the crustal dichotomy boundary, Aeolis Mensae, Mars: Journal of Geophysical Research, v. 109, no. E09011, p. 1–20 (doi:10.1029/2004JE002248).

Kochel, R.C., and Peake, R.T., 1984, Quantification of waste morphology in Martian fretted terrain: Journal of Geophysical Research, v. 89, p. C336–C350.

Kreslavsky, M.A., and Head, J.W., 2002, Fate of outflow channel effluents in the northern lowlands of Mars—The Vastitas Borealis Formation as a sublimation residue from frozen ponded bodies of water: Journal of Geophysical Research, v. 107, no. E12, p. 4-1 to 4-25 (doi:10.1029/2001JE001831).

Laskar, J., and Robutel, P., 1993, The chaotic obliquity of the planets: Nature, v. 361, p. 608–612.

Li, H., Robinson, M.S., and Jurdy, D.M., 2005, Origin of Martian northern hemisphere mid-latitude lobate debris aprons: Icarus, v. 176, p. 382–394.

Lucchitta, B.K., 1976, Mare ridges and related highland scarps—Result of vertical tectonism, *in* Proceedings of the Lunar and Planetary Science Conference, 7th: New York, Pergamon Press, Geochimica Et Cosmochimica Acta, Supplement 7, p. 2761–2782.

Lucchitta, B.K., 1977, Topography, structure, and mare ridges

in southern Mare Imbrium and northern Oceanus Procellarum, *in* Proceedings of the Lunar and Planetary Science Conference, 8th: New York, Pergamon Press, Geochimica Et Cosmochimica Acta, Supplement 8, p. 2691–2703.

Lucchitta, B.K., 1978, Geologic map of the Ismenius Lacus quadrangle of Mars: U.S. Geological Survey Miscellaneous Investigations Map I–1065, scale 1:5,000,000.

Lucchitta, B.K., 1984, Ice and debris in the fretted terrain, Mars, *in* Proceedings of the Lunar and Planetary Science Conference, 14th: Journal of Geophysical Research, v. 89, supplement, no. S2, p. B409–B418.

Malin, M.C., and Edgett, K.S., 1999, Oceans or seas in the Martian northern lowlands—High resolution imaging tests of proposed shorelines: Geophysical ResearchLetters, v. 26, p. 3049–3052.

Malin, M.C., and Edgett, K.S., 2001, Mars Global Surveyor Mars Orbiter Camera— Interplanetary cruise through primary mission: Journal of Geophysical Research, v. 106, no. E10, p. 23429–23570 (doi:10.1029/2000JE001455).

Mangold, N., 2003, Geomorphic analysis of lobate debris aprons on Mars at Mars Orbiter Camera scale—Evidence for ice sublimation initiated by fractures: Journal of Geophysical Research, v. 108, no. E4, p. 2-1 to 2-13 (doi:10.1029/2002JE001885).

Mangold, N., and Allemand, P., 2001, Topographic analysis of features related to ice on Mars: Geophysical Research Letters, v. 28, p. 407–410.

McCauley, J.F., Carr, M.H., Cutts, J.A., Hartmann, W.K., Masursky, H., Milton, D.J., Sharp, R.P., and Wilhems, D.E., 1972, Preliminary Mariner 9 report on the geology of Mars: Icarus, v.17, p. 289–327.

McGill, G.E., 1989, Buried topography of Utopia, Mars—Persistence of a giant impact depression: Journal of Geophysical Research, v. 94, p. 2753–2759.

McGill, G.E., 2000, Crustal history of north central Arabia Terra, Mars: Journal of Geophysical Research, v. 105, p. 6945–6959.

McGill, G.E., 2001, The Utopia basin revisited—Regional slope and shorelines from MOLA profiles: Geophysical Research Letters, v. 28, p. 411–414.

McGill, G.E., 2002, Geologic map transecting the highland/lowland boundary zone, Arabia Terra, Mars—Quadrangles 30332, 35332, 40332, and 45332: U.S. Geological Survey Geologic Investigations Series Map I–2746, scale 1:1,000,000.

McGill, G.E., and Dimitriou, A.M., 1990, Origin of the Martian global dichotomy by crustal thinning in the Late Noachian or Early Hesperian: Journal of Geophysical Research, v. 95, p. 12,595–12,605.

McGill, G.E., and Squyres, S.W., 1991, Origin of the Martian crustal dichotomy—Evaluating hypotheses: Icarus, v. 93, p. 386–393.

Mellon, M.T., and Jakosky, B.M., 1993, Geographic variations in the thermal and diffusive stability of ground ice on Mars: Journal of Geophysical Research, v. 98, p. 3345–3364.

Melosh, H.J., 1989, Impact cratering, a geologic process: New York, Oxford University Press, 245 p.

Milliken, R.E., Mustard, J.F., and Goldsby, D.L., 2003, Viscous flow features on the surface of Mars—Observations from high-resolution Mars Orbiter Camera (MOC) images: Journal of Geophysical Research, v. 108, no. E6 (doi:10.1029/2002JE002005).

Mouginis-Mark, P.J., 1987, Water or ice in the Martian regolith?—Clues from Rampart craters seen at very high resolution: Icarus, v. 71, p. 268–286.

Mustard, J.F., Cooper, C.D., and Rifkin, M.K., 2001, Evidence for recent climate change on Mars from the identification of youthful near-surface ground ice: Nature, v. 412, p. 411–414.

Newsom, H.E, 1980, Hydrothermal alteration of impact melt sheets with implications for Mars: Icarus, v. 44, p. 207–216.

Nimmo, F., and Tanaka, K., 2005, Early crustal evolution of Mars: Annual Reviews of Earth and Planetary Science, v. 33, p. 133–161.

Nummedal, D., and Prior, D.B., 1981, Generation of Martian chaos and channels by debris flows: Icarus, v. 45, p. 77–86.

Parker, T.J., Gorsline, D.S., Saunders, R.S., Pieri, D.C., and Schneeberger, D.M., 1993, Coastal geomorphology of the Martian northern plains: Journal of Geophysical Research, v. 98, p. 11,061–11,078.

Parker, T.J., Saunders, R.S., and Schneeberger, D.M., 1989, Transitional morphology in West Deuteronilus Mensae, Mars—Implications for modification of the lowland/upland boundary: Icarus, v. 82, p. 111–145.

Perron, J.T., Mitrovica, J.X., Manga, M., Matsuyama, I., and Richards, M.A., 2007, Evidence for an ancient Martian ocean in the topography of deformed shorelines: Nature, v. 447, p. 840–843.

Pierce, T.L., and Crown, D.A., 2003, Morphologic and topographic characteristics of debris aprons in the eastern Hellas region, Mars: Icarus, v. 163, p. 46–65.

Plescia, J.B., and Golombek, M.P., 1986, Origin of planetary wrinkle ridges based on the study of terrestrial analogs: Geological Society of America Bulletin, v. 97, p. 1289–1299.

Rodriguez, J.A.P., Sasaki, S., Kuzmin, R.O., Dohm, J.M., Tanaka, K.L., Miyamoto, H., Kurita, K., Komatsu, G., Fairén, A.G., and Ferris, J.C., 2005, Outflow channel sources, reactivation, and chaos formation, Xanthe Terra, Mars: Icarus, v. 175, p. 36–57.

Rodriguez, J.A.P., Tanaka, K.L., Miyamoto, H., and Sasaki, S., 2006, Nature and characteristics of the flows that carved the Simud and Tiu outflow channels, Mars: Geophysical Research Letters, v. 33, no. L08S04, p. 1–5 (doi:10.1029/2005GL024320)

Rotto, S., and Tanaka, K.L., 1995, Geologic/geomorphologic map of the Chryse Planitia region of Mars: U.S. Geological Survey Miscellaneous Investigations Map I–2441, scale 1:5,000,000.

Schonfeld, E., 1979, Origin of Valles Marineris, *in* Lunar and Planetary Science Conference, Proceedings, 1989: Houston, Tex., Lunar and Planetary Institute, v. 10, p. 3031–3038.

Schultz, R.A., and Frey, H.V., 1990, A new survey of large

multiring impact basins on Mars: Journal of Geophysical Research, v. 95, p. 14,175–14,189.
Schultz, R.A., and Gault, D.E., 1979, Atmospheric effects on Martian ejecta emplacement: Journal of Geophysical Research, v. 84, p. 7,669–7,687.
Scott, D.H., Dohm, J.M., and Rice, J.W., 1995, Map of Mars showing channels and possible paleolake basins: U.S. Geological Survey Miscellaneous Investigations Series Map 2461, scale 1:30,000,000.
Seidelmann, P.K., Abalakin, V.K., Bursa, M., Davies, M.E., De Bergh, C., Lieske, J.H., Oberst, J., Simon, J.L., Standish, E.M., Stooke, P., and Thomas, P.C., 2002, Report of the IAU/IAG working group on cartographic coordinates and rotational elements of the planets and satellites—2000: Celestial Mechanics and Dynamics of Astronomy, v. 82, p. 83–110.
Sharp, R.P., 1973a, Fretted and chaotic terrain: Journal of Geophysical Research, v. 78, p. 4073–4083.
Sharp, R.P., 1973b, Troughed terrain: Journal of Geophysical Research, v.78, p. 4063–4072.
Sharp, R.P., and Malin, M.C., 1975, Channels on Mars: Geological Society of America Bulletin, v. 86, p. 593–609.
Skinner, J.A., Tanaka, K.L., Hare, T.M., Kargel, J., Neukum, G., Werner, S.C., and Rodriguez, J.A.P., 2004, Mass-wasting of the circum-Utopia highland/lowland Boundary—Processes and controls [abs.], *in* Workshop on Hemispheres apart— The origin and modification of the Martian crustal dichotomy, Houston, Tex., Sept. 30–Oct. 1, 2004: Houston, Tex., Lunar and Planetary Institute, no. 4019.
Sleep, N.H., 1994, Martian plate tectonics: Journal of Geophysical Research, v. 99, p. 5639–5656.
Sleep, N.H., 2000, Evolution of the mode of convection within terrestrial planets: Journal of Geophysical Research, v. 105, 17,563–17,578.
Solomon, S.C., Aharonson, O., Aurnou, J.M., Banerdt, B.W., Carr, M.H., Dombard, A.J.,Frey, H.V., Golombek, M.P., Hauck, S.A., Head, J.W., Jakosky, B.M., Johnson, C.L., McGovern, P.J., Neumann, G.A., Phillips, R.J., Smith, D.E., and Zuber, M.T., 2005, New perspectives on ancient Mars: Science, v. 307, p. 1214–1220.
Squyres, S.W., 1978, Martian fretted terrain—Flow of erosional debris: Icarus, v. 34, p. 600–613.
Squyres, S.W., 1979, The distribution of lobate debris aprons and similar flows on Mars: Journal of Geophysical Research, v. 84, p. 8087–8096.
Squyres, S.W., 1989, Urey prize lecture: Water on Mars: Icarus, v. 79, p. 229–288.
Squyres, S.W., and Carr, M.H., 1986, Geomorphic evidence for the distribution of ground ice on Mars: Science, v. 231, p. 249–252.
Tanaka, K.L., 1986, The stratigraphy of Mars, *in* Proceedings of the Lunar and Planetary Science Conference, 17th, Part 1, November, 1986: Journal of Geophysical Research, v. 91, supplement, no. B13, p. E139–158.
Tanaka, K.L., and Golombek, M.P., 1989, Martian tension fractures and the formation of grabens and collapse features at Valles Marineris, *in* Lunar and Planetary Science Conference, Proceedings, 1989: Houston, Tex., Lunar and Planetary Institute, v. 19, p. 383–396.
Tanaka, K.L., Scott, D.H., and Greeley, R., 1992, Global stratigraphy, *in* Kiefer, H.H., Jakosky, B.M., Snyder, C.W., and Mathews, M.S., eds., Mars: Tucson, Ariz., University of Arizona Press, p. 345–482.
Tanaka, K.L., Skinner, J.A., and Hare, T.M., 2005, Geologic map of the northern plains of Mars: U.S. Geological Survey Scientific Investigations Series Map 2888, scale 1:15,000,000.
Tanaka, K.L., Skinner, J.A., Hare, T.M., Joyal, T., and Wenker, A., 2003, Resurfacing history of the northern plains of Mars based on geologic mapping of Mars Global Surveyor data: Journal of Geophysical Research, v. 108, no. E4 (doi:10.1029/2002JE001908).
Thomson, B.J., and Head, J.W., III, 1999, Utopia Basin, Mars––A new assessment using Mars Orbiter Laser Altimeter (MOLA) data [abs.]: Houston, Tex., Lunar and Planetary Institute, Lunar and Planetary Science Conference, XXX, Abstract no. 1894 [CD-ROM].
Touma, J., and Wisdom, J., 1993, The chaotic obliquity of Mars: Science, v. 259, p. 1294–1297.
Turtle, E.P., Pathare, A.V., Crown, D.A., Chuang, F.C., Hartmann, W.K., Greenham, J.C., and Bueno, N.F., 2003, Modeling the deformation of lobate debris aprons on Mars by creep of ice-rich permafrost [abs.]: International Conference on Mars Polar Science and Exploration, 3rd, Alberta, Canada, Oct. 13–17, no. 8091.
Watters, T.R., 1988, Wrinkle ridge assemblages on the terrestrial planets: Journal of Geophysical Research, v. 93, p. 10,236–10,254.
Watters, T.R., 1991, Origin of periodically spaced wrinkle ridges on the Tharsis plateau of Mars: Journal of Geophysical Research, v. 96, p. 15,599–15,616.
Watters, T.R., 1993, Compressional tectonism on Mars: Journal of Geophysical Research, v. 98, p. 17,049–17,060.
Watters, T.R., and McGovern, P.J., 2006, Introduction to special section—The hemispheric dichotomy of Mars: Geophysical Research Letters, v. 33, no. L08S01, p. 1–4 (doi:10.1029/2006GL025755).
Webb, V.E., 2004, Putative shorelines in northern Arabia Terra, Mars: Journal of Geophysical Research, v.109, no. E09010, p. 1–12 (doi:10.1029/2003JE002205).
Wilhelms, D.E., and Squyres, S.W., 1984, The Martian hemispheric dichotomy may be due to a giant impact: Nature, v. 309, p. 138–140.
Williams, D.A., and Greeley, R., 1994, Assessment of antipodal-impact terrains on Mars: Icarus, v. 110, p. 196–202.
Wise, D.U., Golombek, M.P., and McGill, G.E., 1979, Tharsis province of Mars— Geologic sequence, geometry, and a deformation mechanism: Icarus, v. 38, p. 456–472.
Withers, P., and Neumann, G.A., 2001, Enigmatic northern plains of Mars: Nature, v. 410, p. 651.
Zhong, S.J., and Zuber, M.T., 2001, Degree-1 mantle convection and the crustal dichotomy of Mars: Earth and Planetary Science Letters, v. 189, p. 75–84.
Zimbelman, J.R., Clifford, S.M., and Williams, S.H., 1989, Concentric crater fill on Mars—An aeolian alternative to ice-rich mass wasting, *in* Lunar and Planetary Science

Conference, Proceedings, 1989: Houston, Tex., Lunar and Planetary Institute, v. 19, p. 397–407.
Zuber, M.T., 1995, Wrinkle ridges, reverse faulting, and the depth penetration of lithospheric strain in Lunae Planum: Icarus, v. 114, p. 80–92.
Zuber, M.T., 2001, The crust and mantle of Mars: Nature, v. 412, p. 220–227.
Zuber, M.T., Solomon, S.C., Phillips, R.J., Smith, D.E., Tyler, G.L., Aharonson, O., Balmino, G., Banerdt, W.B., Head, J.W., Johnson, C.L., Lemoine, F.G., McGovern, P.J., Neumann, G.A., Rowlands, D.D., and Zhong, S., 2000, Internal structure and early thermal evolution of Mars from Mars Global Surveyor topography and gravity: Science, v. 287, p. 1788–1793.

Table 1. *Crater Size-Frequency Data and Relative Age Determinations*

[Craters counted using Viking MDIM, THEMIS daytime IR, and HRSC data (see fig. 2, Data and GIS Mapping Techniques section for more details). N(2), N(5), and N(16) represent the cumulative number of craters ≥ 2, 5, and 16 km in diameter normalized to 10^6 km^2; only cumulative totals > 4 are used to determine ages. Error = ±((N0.5)/A) x 10^6 km^2, where A = area. Age ranges are based upon crater counts using the crater-density boundaries by Tanaka (1986); EA, Early Amazonian; MA, Middle Amazonian; LA, Late Amazonian; EH, Early Hesperian; LH, Late Hesperian; EN, Early Noachian; MN, Middle Noachian; LN, Late Noachian]

Unit Name	Unit label	Area (km^2)[1]	No. ≥ 0.5 km	No. ≥ 2 km	No. ≥ 5 km	No. ≥ 16 km	N(2)	N(5)	N(16)	N(2) age range	N(5) age range	N(16) age range	Relative Age[2]
Smooth fill material	Afs	5285	6	0	0	0	---	---	---	---	---	---	EA-LA
Debris apron material	Ada	43089	31	7	0	0	162±61	---	---	EA-MA	---	---	EA-MA
Well-preserved crater material	c_3	11664	66	4	0	0	---	---	---	---	---	---	LH-EA
Moderately degraded crater material	c_2	10036	21	3	1	0	---	---	---	---	---	---	EH-LH
Highly degraded crater material	c_1	2524	11	0	0	0	---	---	---	---	---	---	MN-EH
Mottled plains material	Hpm	8015	20	5	2	0	624±279	---	---	EH-EA	---	---	EH-LH
Smooth plains material	HNps	33917	115	28	9	1	825±156	265±88	---	EH-LH	LN-EH	---	LN-EH
Cerulli crater material	Ncc	26510	255	22	10	3	830±177	377±119	---	EH-LH	≥ LN	---	MN-LN
Dissected plateau material	Npld	19667	247	24	12	0	1220±249	610±176	---	LN-EH	≥ MN	---	≥ MN
Upper smooth plateau material	Nplsu	45935	394	68	31	10	1480±179	675±121	218±69	≥ LN	≥ MN	≥ MN	≥ MN
Lower smooth plateau material	Nplsl	4766	10	1	0	0	---	---	---	---	---	---	≥ MN

[1]Estimated using sinusoidal equal-area projection with a spherical shape definition for Mars (axes=3396190 m).

[2]Relative age range is primarily based on measured crater densities (where available), with adjustments from observed stratigraphic relationships (see table 2 for contact relations). N(5) ranges are favored for highland plateau units as N(2) ranges may reflect younger surface modification. Note that these ranges may differ slightly from those in the Correlation of Map Units, which represent inferences from a synthesis of regional geologic history.

Table 2. *Contact Relations of Geologic Units*

Unit Name	Unit label	Contact relations[1] Younger than	Overlaps with[2]	Older than
Smooth fill material	Afs	Nplsu, Npld, Ncc, c_1, c_2, c_3	Ada	---
Debris apron material	Ada	Nplsu, Nplsl, Npld, Hpm, HNps, c_1, c_2, c_3	Afs	---
Well-preserved crater material	c_3	HNps, Npld, Nplsu	c_2	Ada, Afs
Moderately degraded crater material	c_2	c_1, Hpm, HNps, Ncc, Npld, Nplsu, Nplsl	c_3	Ada, Afs
Highly degraded crater material	c_1	Nplsu, Nplsl, Npld, Ncc	---	Ada, Afs, c_2, Hpm, HNps
Mottled plains material	Hpm	c_1, Nplsu, Nplsl, HNps	---	Ada, c_2
Smooth plains material	HNps	c_1, Nplsu, Nplsl	---	Ada, Hpm, c_2, c_3
Cerulli crater material	Ncc	Nplsu, Npld	---	c_1, c_2, Afs
Dissected plateau material	Npld	---	Nplsu, Nplsl	Ada, Afs, Ncc, c_1, c_2, c_3
Upper smooth plateau material	Nplsu	Nplsl	Npld	Ada, Hpm, HNps, c_1, c_2
Lower smooth plateau material	Nplsl	---	Npld	Ada, Afs, Hpm, HNps, Ncc, Nplsu, c_1, c_2, c_3

[1]Contact relations are for units that share in common, one or more geologic contacts.
[2]Exhibits one or more locations where contacts between units are topographically or stratigraphically equivalent.